DokumentID
1713264, (1.0 Godkänt)
Reg nr

Sekretess
Öppen
Dokumenttyp
Memo

Sida
1(20)

Författare
2019-04-04 Johannes Johansson

Corrosion of copper in repository-like field tests: compilation and analysis of data

Content

1 Introduction

Field tests of repository-like installations offer the possibility to study the integrated development of the engineered barrier system on different time scales. The strength of field tests is that they can be set up to illustrate a realistic initial development of a KBS-3 repository, which can be used for example to validate models and the conceptual understanding of the development of the system. On the other hand, field tests have a at least two weaknesses in that 1) the establishment of long-time reducing and sulfidic conditions at the canister-bentonite interface might take years if the bentonite barrier is dense and thick enough, and 2) parameter control is difficult to achieve without disturbing the system's natural development. For these reasons, the detailed mechanistic understanding of the development of the corrosion process must be approached using controlled laboratory experiments and theoretical modeling. SKB and other waste management organizations have conducted a number of field tests of the KBS-3 barrier system from which data have been obtained and conceptual understanding can be gained. In this Memo, the outcome of these field tests, with focus on the corrosion data gathered, will be analyzed and discussed.

In the corrosion model applied in SKB's safety assessments for a KBS-3 repository at the Forsmark site, the initial corrosion of copper is due to residual oxygen from the air saturated bentonite porosity and air-filled macroscopic voids in the near field, for example the gap present initially between the bentonite blocks and the copper canister. When the residual oxygen has been consumed by corrosion of copper and other oxidation processes in the near field, gamma radiolysis of water continues to cause some further corrosion of the canister until the sulfidic ground water has saturated the bentonite clay and transport-controlled corrosion by sulfide continues (King et al. 2013, 2017). Since the concentration of sulfide in the ground water is low, and since diffusion through the bentonite is slow, the residual oxygen present from the start dominates the corrosion observed in typical field tests.

In this Memo, four of SKB's field tests performed at the Äspö Hard Rock Laboratory (HRL) will be described, including the experimental configurations, the initial conditions of the tests and what is known about the development of the redox conditions. A field test performed by Enresa (Spain) and NAGRA (Switzerland) at the Grimsel test-site in Switzerland will also be described since copper corrosion data was available for comparison. The corrosion observed visually and spectroscopically in these field tests will be reviewed and it is discussed how the observations may be understood from the initial state and development of the redox conditions. The available test data, such as residual oxygen, temperature, and exposure time, will be analyzed to see what conclusions can be drawn and which parameters control the corrosion depth in these tests. The overall aim of this Memo is to examine how the corrosion model applied in SKB's safety assessments corresponds with the early development of corrosion observed in these field tests.

2 Description of the experiments

The following field tests performed at the Äspö HRL, will be described and discussed herein: Prototype Repository (PR), Long-term test of buffer materials (LOT), Alternative Buffer Materials (ABM), and In situ corrosion test of miniature canisters (MiniCan). Reference will also be made to the Full-scale Engineered Barrier Experiment in Crystalline Host Rock (Febex), performed by Enresa and NAGRA at the Grimsel site.

2.1 Prototype repository (PR)

The full scale field experiment Prototype Repository (PR) represents the initial phase and early environmental development of a future KBS-3 repository. The canisters are five meters high and consist of a five cm thick copper shell and a cast iron insert, which is the reference canister design. The copper shell was made of SKB's reference material, oxygen-free phosphorous doped copper

(Cu-OFP). The installation consists of a horizontal tunnel at 450 m depth, in which six copper canisters have been emplaced in vertical deposition holes. The deposition holes are eight meters deep and just less than two meters in diameter. The canisters are surrounded by 35 cm thick bentonite rings and cylindrical bentonite blocks fill the top and bottom of a deposition hole, see Figure 1. The horizontal tunnel was divided into an inner and an outer section, containing four (PR1-PR4) and two canisters (PR5 and PR6), respectively (Figure 1). Each section was backfilled with bentonite clay and sealed with a concrete plug, the inner section in 2001 and the outer in 2003. In 2011 the outer section of the experiment was opened and the canisters PR5 and PR6 were retrieved and analysed after eight years of exposure in the Äspö HRL. Further details of the experimental configuration of PR can be found in Svemar et al. (2016).

In order to simulate the thermal effect of the encapsulated spent nuclear fuel, the canisters were equipped with heaters, started shortly after installation. The aim of PR was to study the behaviour of the integrated rock-bentonite-canister system with primary focus on the bentonite buffer. Therefore, the experiment is not optimal for studying copper corrosion; the initial state of the canister surfaces was not characterised, and there were no mass-loss specimens mounted in the clay. However, electrochemical monitoring of corrosion rates was performed on cylindrical copper electrodes installed in bentonite blocks above the canisters in PR1 (block C3) and PR5 (block C4). Technical details of these measurements are given in Rosborg (2013a).

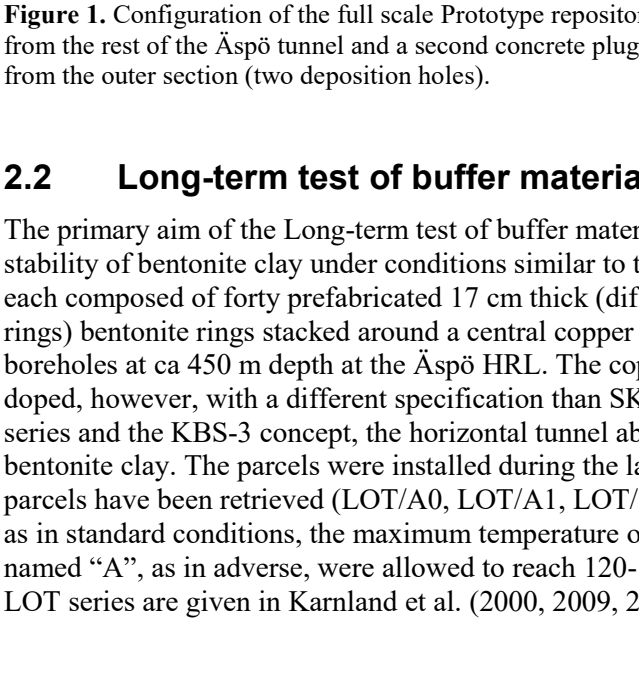

Figure 1. Configuration of the full scale Prototype repository. Initially, a concrete plug sealed the experiment from the rest of the Äspö tunnel and a second concrete plug divided the inner section (four deposition holes) from the outer section (two deposition holes).

2.2 Long-term test of buffer material (LOT)

The primary aim of the Long-term test of buffer material (LOT) was to study the mineralogical stability of bentonite clay under conditions similar to those in a KBS-3 repository. Seven test parcels, each composed of forty prefabricated 17 cm thick (difference between outer and inner diameter of the rings) bentonite rings stacked around a central copper tube, were deposited in 4 m deep vertical boreholes at ca 450 m depth at the Äspö HRL. The copper quality was oxygen-free and phosphorous doped, however, with a different specification than SKB's reference material. In contrast to the PR series and the KBS-3 concept, the horizontal tunnel above the LOT boreholes was not backfilled with bentonite clay. The parcels were installed during the late 1990's and to date (April, 2019) four test parcels have been retrieved (LOT/A0, LOT/A1, LOT/S1, and LOT/A2). In the packages named "S", as in standard conditions, the maximum temperature of the heaters were 90 °C, while the packages named "A", as in adverse, were allowed to reach 120-150 °C during the test. Further details of the LOT series are given in Karnland et al. (2000, 2009, 2011).

In order to quantify the extent of copper corrosion, each of the test parcels contains copper coupons of accurately known initial weights in bentonite rings 22 and 30 (Figure 2). In addition, a set of three cylindrical copper electrodes were installed in bentonite ring 36 of test parcel A2, which allows real-time electrochemical monitoring of corrosion (Rosborg et al. 2004, Rosborg 2013a). As for the PR test series, the copper tubes in LOT were equipped with internal 2 kW heaters to simulate the thermal effect of the spent nuclear fuel. Since mineralogical transformations can be sensitive to temperature variations, the distribution of the thermal field in the bentonite clay was monitored during exposure, which allows specification of the temperatures at the positions of the copper coupons.

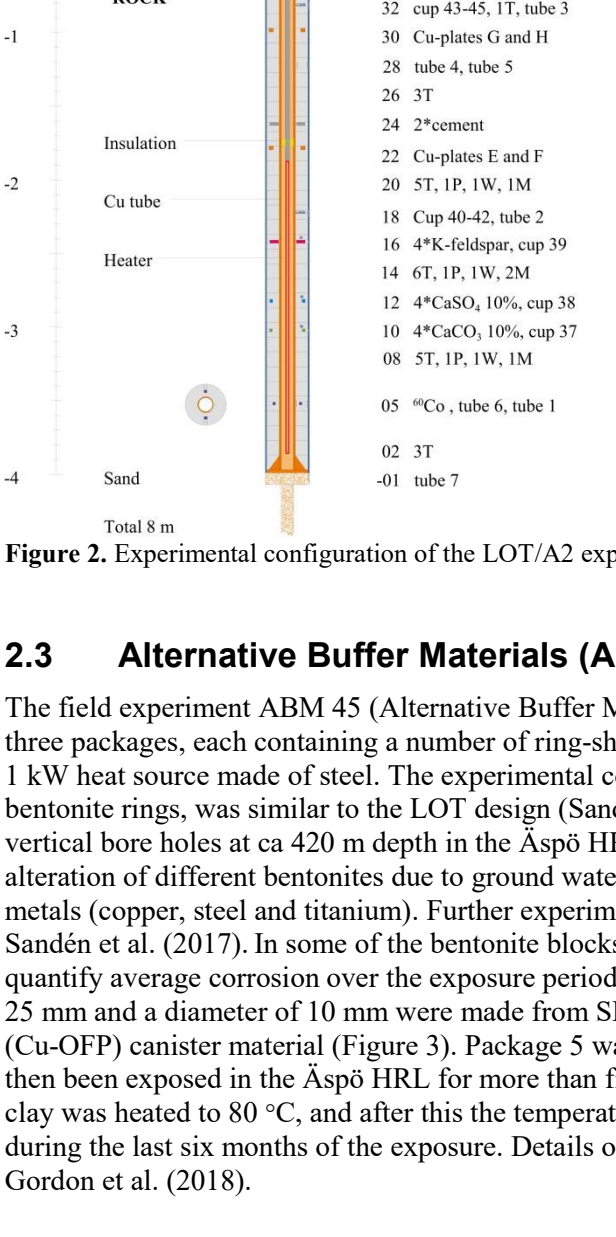

Figure 2. Experimental configuration of the LOT/A2 experiment.

2.3 Alternative Buffer Materials (ABM)

The field experiment ABM 45 (Alternative Buffer Materials package 4, 5, and 6) consisted initially of three packages, each containing a number of ring-shaped bentonite blocks stacked around a cylindrical 1 kW heat source made of steel. The experimental configuration, e.g. the diameter and thickness of the bentonite rings, was similar to the LOT design (Sandén et al. 2017). The packages were installed in vertical bore holes at ca 420 m depth in the Äspö HRL and the aim of the test was to study the alteration of different bentonites due to ground water saturation, heating and interaction with corroding metals (copper, steel and titanium). Further experimental details of the ABM series can be found in Sandén et al. (2017). In some of the bentonite blocks, copper specimens were installed with the aim to quantify average corrosion over the exposure period. Cylindrical copper specimens with a height of 25 mm and a diameter of 10 mm were made from SKB's oxygen-free phosphorous doped copper (Cu-OFP) canister material (Figure 3). Package 5 was retrieved during the autumn of 2017 and had by then been exposed in the Äspö HRL for more than five years. For the first four and a half years, the clay was heated to 80 °C, and after this the temperature was increased to between 150 and 250 °C during the last six months of the exposure. Details of the corrosion examination can be found in Gordon et al. (2018).

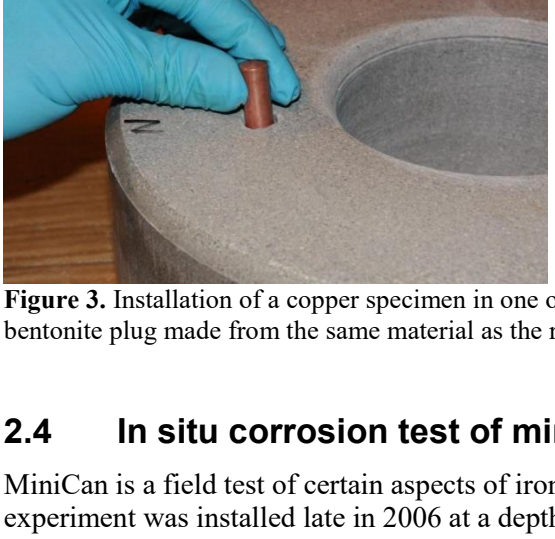

Figure 3. Installation of a copper specimen in one of the bentonite rings in ABM. The hole was sealed with a bentonite plug made from the same material as the ring.

2.4 In situ corrosion test of miniature canisters (MiniCan)

MiniCan is a field test of certain aspects of iron and copper corrosion in a KBS-3 type repository. The experiment was installed late in 2006 at a depth of 450 m in the Äspö HRL. Initially the test contained five experimental packages, differing in various ways but most importantly regarding the presence and density of the bentonite clay surrounding the miniature copper-cast iron canisters (Smart and Rance 2009). In the MiniCan experiment, the copper-cast iron canisters were mounted inside stainless steel cages, which held the bentonite clay in place in the nearly horizontal bore holes that were filled with ground water. This is in contrast to the design of the KBS-3 repository, in which the copper-cast iron canisters will be installed directly in the boreholes with high density bentonite clay filling the space between canister and rock.

In the MiniCan packages 1-3, the canisters were surrounded by low density (1300 kg/m^3 dry density) bentonite made from pellets, spatially separated from the canister by an inner steel cage and a sintered steel filter with 10 µm pores. The clay was thus not in direct contact with the canister and served the function of chemically conditioning the incoming ground water only. The steel cage was isolated from the copper canister by a plastic ribbon to avoid galvanic coupling of the metals. In package 4 the canister was embedded in 3 cm thick bentonite rings of high density (1600 kg/m^3 dry density) in direct contact with the copper surface (Figure 4). In package 5, no bentonite was present in the steel cage, and the copper surface was exposed directly to the ground water. In the void volume inside the steel cage (on top of the copper canister, which was shorter than the steel cage, see Figure 4), electrodes and corrosion specimens of both iron and copper were installed on a nylon rack and were isolated from each other. Further details of the design of the MiniCan test series are described in Smart and Rance (2009). MiniCan 3 was retrieved in 2011 and packages 4 and 5 were retrieved in 2015. During post-test examination it was found that microbial sulfate reduction had a pronounced influence on the corrosion of cast iron components in both MiniCan 3 (low density bentonite) and 5 (no bentonite). As a result, most surfaces in these packages, copper specimens included, were covered with a black deposit consisting partly of iron sulfides (Smart and Rance 2009, Smart et al. 2012, Gordon et al. 2017).

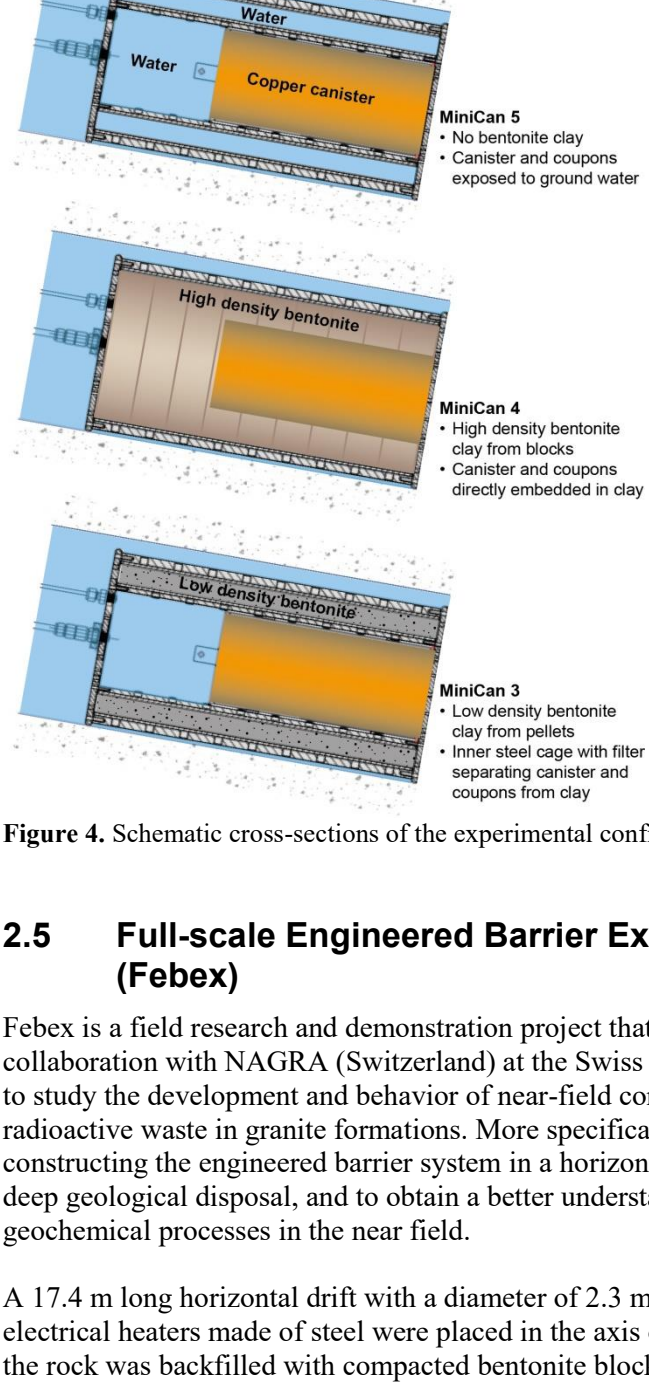

Figure 4. Schematic cross-sections of the experimental configurations of MiniCan 3, 4, and 5.

2.5 Full-scale Engineered Barrier Experiment in Crystalline Host Rock (Febex)

Febex is a field research and demonstration project that is conducted by Enresa (Spain) in collaboration with NAGRA (Switzerland) at the Swiss Grimsel Test Site (GTS). The aim of Febex is to study the development and behavior of near-field components in a repository for high-level radioactive waste in granite formations. More specifically, it is a demonstration of the feasibility of constructing the engineered barrier system in a horizontal configuration, as in the Spanish concept for deep geological disposal, and to obtain a better understanding of the thermo-hydro-mechanical and geochemical processes in the near field.

A 17.4 m long horizontal drift with a diameter of 2.3 m was excavated in the Grimsel rock. Two electrical heaters made of steel were placed in the axis of the drift. The gap between the heaters and the rock was backfilled with compacted bentonite blocks, requiring nearly 116 tons of bentonite. The backfilled area was sealed with a concrete plug. A more detailed and illustrated description of Febex is found in Lanyon and Gaus (2016). The experiment was started in 1997 and was carried out in two phases, so that the outer section and its heater were retrieved in 2002, and the inner section was retrieved during 2015. Several instruments were mounted in the experimental zone, both in the bentonite buffer and in the host rock, to monitor parameters such as temperature, humidity, pressure, displacements, ground water chemistry, and redox development. Amongst the instruments and test specimens were two copper coupons from the inner section, mounted on a plastic rack near the central heater and heated to around 100 °C during the 18 year long exposure.

3 Results and discussion

3.1 Residual O_2 and development of redox conditions

The amount of residual oxygen available is determined by the volume, porosity, and water content of the bentonite clay at installation. Since the bentonite blocks are produced under aerobic conditions it can be assumed that the porosity and the pore water are saturated with air. The porosity of compacted bentonite blocks is typically around 0.4, and ca 65 % of the pore volume is filled with water, giving a remaining air-filled porosity of 0.14. Thus, since air contains 20.9 % molecular oxygen, and since the molar volume of an ideal gas is 0.0232 m^3/mol, 1 m^3 bentonite clay contains ca 1.3 moles of O_2. In this calculation of the molar volume of an ideal gas a rock temperature of 10 °C was assumed, since this is a typical temperature in the bedrock at Äspö HRL and since heating in PR, LOT and ABM was started after installation and closure of the test. For comparison, the water filled fraction of the porosity contains ca 0.065 mol O_2 per m^3 bentonite, i.e. a minor contribution compared with the O_2 from the air filled porosity.

PR has the same dimensions as the KBS-3 reference design, in which each deposition hole contains 16.3 m^3 bentonite and thus ca 21 moles of O_2. An additional contribution of ca 7 moles of O_2 comes from the initially air-filled gap of ca 1 cm between the canister and the bentonite rings. In addition, there is in principle an additional amount of 455 moles of O_2 per canister, if the total amount of oxygen in the backfill is divided equally between the canisters (SKB 2010).

The corrosion potential (E_{corr}) of the copper electrode in PR5 was measured just before retrieval of the outer section of PR and was then found to vary between -30 and -60 mV (SHE) (Rosborg 2013b). This can be compared to the E_{corr} of ca 220-260 mV (SHE), obtained for copper electrodes embedded in a bentonite test parcel in an aerobic laboratory environment for several years (Rosborg et al. 2012), suggesting that oxygen had been depleted during the seven years of exposure of the electrode in PR. Important to note though, the E_{corr} of copper is also sensitive to variations in the concentration of chloride. The E_{corr} measured before retrieval can also be compared with E_{corr} for copper electrodes in anoxic sulfide solutions which has been determined in laboratory tests to be -400 mV (SHE) or even lower (depending on the sulfide concentration) in anoxic sulfide solutions (Smith et al. 2004, 2007a, b). This indicates that although the outer section of PR (Figure 1) had been depleted of residual oxygen, it had still not become fully reducing, i.e. the sulfidic ground water of the Äspö site had not yet conditioned the chemistry of the clay. This conclusion is further supported by the examination of corrosion products in PR, discussed below in Section 3.2.

Table 1. Initial state and development of parameters controlling the early corrosion in repository-like field tests performed in the Äspö HRL. For LOT and MiniCan the corrosion depth was determined by mass-loss. For PR the corrosion depth was not measured by mass-loss but was instead estimated by integration of electrochemical measurements of corrosion rates (see further Rosborg 2013a).

Experiment	Prototyp 5	LOT A2	MiniCan 4
Bentonite buffer volume (m^3)	16.3	0.24	0.008
Initial air filled gap between copper and clay (mm)	10	8	-
Initial free water volume (m^3)	-	-	0.4
Residual O_2 (moles)	28	0.8	0.1
Temperature (°C)	35	30	15
Exposure time (y)	7	6	8
Copper specimen	Electrode C4	Coupon 30G	Coupon M4 7:1
Corrosion products	Cu_2O $Cu_2(OH)_2CO_3$	Cu_2O $Cu_2(OH)_3Cl$	Cu_2O Cu_2S
Corrosion depth (µm)	2.8-5.6	2.5	0.2

In LOT, each test hole contains 0.24 m^3 bentonite and thus 0.3 moles of O_2. A contribution of 0.5 moles of O_2 comes from the initially air-filled gap of 0.4 cm between the copper tube and the bentonite rings. No measurements of redox or corrosion potentials were made in LOT; however, a laboratory test has recently been made in which a copper heater was embedded in bentonite rings of similar dimensions as in LOT and ABM, i.e. 17 cm thick rings. The whole experimental package was contained in a stainless steel vessel. These tests showed that residual oxygen, initially comprising 21 % of the gas-phase, fell to about 1 % within 60 days of exposure with the copper heater present. The copper heater then had a maximum temperature of 80 °C. In this test the copper surface was initially washed with hydrochloric acid to remove surface contaminants and grease; however, when instead washing the copper surface with ethanol and repeating the test, consumption of O_2 was ca 5 times slower. At the time of writing the test has not been terminated but as it seems from the online measurements it will take up to 10 months for the system to reach below 1% O_2 (Svensson D 2018, personal communication). When the test was repeated at room temperature and without the copper heater, the oxygen level in the gas-phase remained stable at 22 % for 111 days (Birgersson and Goudarzi 2018). These results show that: 1) a heated copper surface is an efficient sink for consumption of O_2 via corrosion of the copper surface, however, the kinetic efficiency depends on the surface treatment, 2) stainless steel is not an efficient sink for O_2 (probably due to passivity of the steel surface), and 3) at low temperature bentonite clay does not react with O_2 or reacts very slowly[1]. Based on these results, it is reasonable to assume that in the heated packages of the LOT series, having a central copper heater, residual oxygen was primarily consumed by copper corrosion within a period of several months. Oxygen consumption was probably slower in the LOT packages of lower temperature. Most likely, O_2 consumption was also slower in the ABM series, in which the central heater was made

[1] The redox reactivity of the clay depends on the amount of pyrite, which varies between different bentonite materials, and also within different batches of the same material.

of steel and the only copper surface was the comparatively small surface of the corrosion specimens mounted in the bentonite rings.

When comparing PR with LOT or ABM, it is important to note that while the electrodes in PR were installed in 35 cm thick bentonite rings (difference between outer and inner diameter of the rings), the copper specimens in LOT and ABM were mounted in 17 cm thick rings. This means that the amount of residual O_2 available for corrosion differed between the tests. Other notable differences between the field tests are: 1) the total metal surface, competing with the corrosion specimens for O_2, 2) the temperature, which varied between and spatially within the tests, 3) the bentonite used (most of the Äspö tests contained SKB's reference clay MX-80, while ABM contained different types), and 4) the time required to reach full water saturation of the bentonite. These variations make direct comparison of the tests complicated and a more precise understanding of O_2 consumption in the different tests would require three dimensional modeling of O_2 diffusion with the actual experimental configuration, bentonite density, water content and temperature of the specific tests.

Each MiniCan borehole contained ca 400 liters of ground water, presumably saturated with air (ca 10 mg O_2 per litre water) when the packages were installed and the boreholes were sealed. Each MiniCan experiment thus contained ca 0.1 mole of O_2 from the water and in addition the packages with clay contained less than $5 \cdot 10^{-3}$ moles of O_2 from the bentonite in which the canister and other corrosion specimens were embedded. It is important to note that the amount of residual oxygen available in the bentonite clay at start was much lower in MiniCan as compared with PR, LOT and ABM (Table 1). MiniCan is the only field test in SKB's regime where both redox- (E_h) and corrosion potentials (E_{corr}) have been measured continuously. The measurements showed that the boreholes became reducing within a few months from closure (Smart et al. 2015). The redox potential (E_h) had by then stabilized at ca -300 mV (SHE) and E_{corr} for copper had converged to around -400 mV (SHE). The corrosion potential in anoxic sulfide solution is controlled by [HS^-] which was in the order of 10^{-6} M in MiniCan during the exposure period, albeit with some variation over time and between the five packages. The E_{corr} values measured in MiniCan are in reasonable agreement with measurements in laboratory experiments, for which E_{corr} was ca -650 mV (SCE) (i.e. -400 mV (SHE)) at [HS^-]=$2.6 \cdot 10^{-5}$ M and decreasing steeply for higher sulfide concentrations (Smith et al. 2004, 2007a, b). For MiniCan 4, directly embedded in high density clay, measurements of E_h in the borehole indicate that it took about one year before the potential stabilized, however, E_{corr} of both the copper canister and other electrodes inside the experimental assembly had stabilized already after ca 4 months (Figure 4-19 in Smart et al. 2015). Due to technical problems with the counter electrode, the development of E_{corr} before 4 months could not be recorded, meaning that the interior of MiniCan 4 might have become depleted of O_2 even earlier than after 4 months.

The amount of residual oxygen at installation of Febex can be estimated from the volume of bentonite clay in the backfilled tunnel (17 m long and 2.2 m in diameter) containing the two heaters (4.5 m long, 1 m in diameter), which corresponds to an amount of ca 57 m^3 clay. Using the same assumptions regarding porosity as for PR this corresponds to an initial amount of ca 74 moles of O_2. Measurements during the test showed that the gas in the bentonite pore system had an atmospheric contain of ca 21 % O_2 at start and that it took ca 1.5 years before the O_2 level decreased to reach low levels (Giroud 2014). The reason for this rather long aerobic period in Febex is not fully understood but it has been suggested that the system was not completely air tight due to cables for instrumentation going through the concrete plug. Furthermore, the clay system was not fully water saturated and some regions were very dry, which allows air and other gases to diffuse rapidly through the system.

3.2 Corrosion products

When the canisters of PR5 and PR6 were retrieved after more than eight years of exposure, large areas were covered with a dark brown deposit, here and there decorated with blue-green regions, indicating that divalent copper corrosion products had formed. By visual inspection, the coupons (LOT/S1, LOT/A0, and LOT/A2) and electrodes (LOT/A2, PR5) mounted in the bentonite clay surrounding the

central canister or tube all had a similar appearance at retrieval (Figure 5a-c). In order to characterize the corrosion products, specimens from PR5 and LOT/A2 have been analysed using x-ray diffraction (XRD), Fourier transformed infra-red spectroscopy (FTIR), Raman spectroscopy, and scanning electron microscopy in combination with energy dispersive spectroscopy (SEM-EDS).

The appearance of the cylindrical electrode in PR5/C4 is shown in Figure 5b. FTIR transmission spectra were dominated by bands from bentonite (Si-O vibrations at 1,000–1,100 cm^{-1} and OH bands at 3,600 cm^{-1}). However, in the spectrum from a brown region of the surface a peak appeared at 620 cm^{-1}, corresponding to cuprite (Cu_2O) (Fig 3-9 in Rosborg 2013b). Similarly, the FTIR spectrum from a blue-green spot revealed several bands matching well with the spectrum of malachite ($Cu_2(OH)_2CO_3$). In agreement with FTIR, XRD spectra revealed the presence of montmorillonite (from bentonite), as well as cuprite and malachite. The Raman spectrum of a blue-green spot matches with malachite ($Cu_2(OH)_2CO_3$) but not with, for example, paratacamite ($Cu_2(OH)_3Cl$).

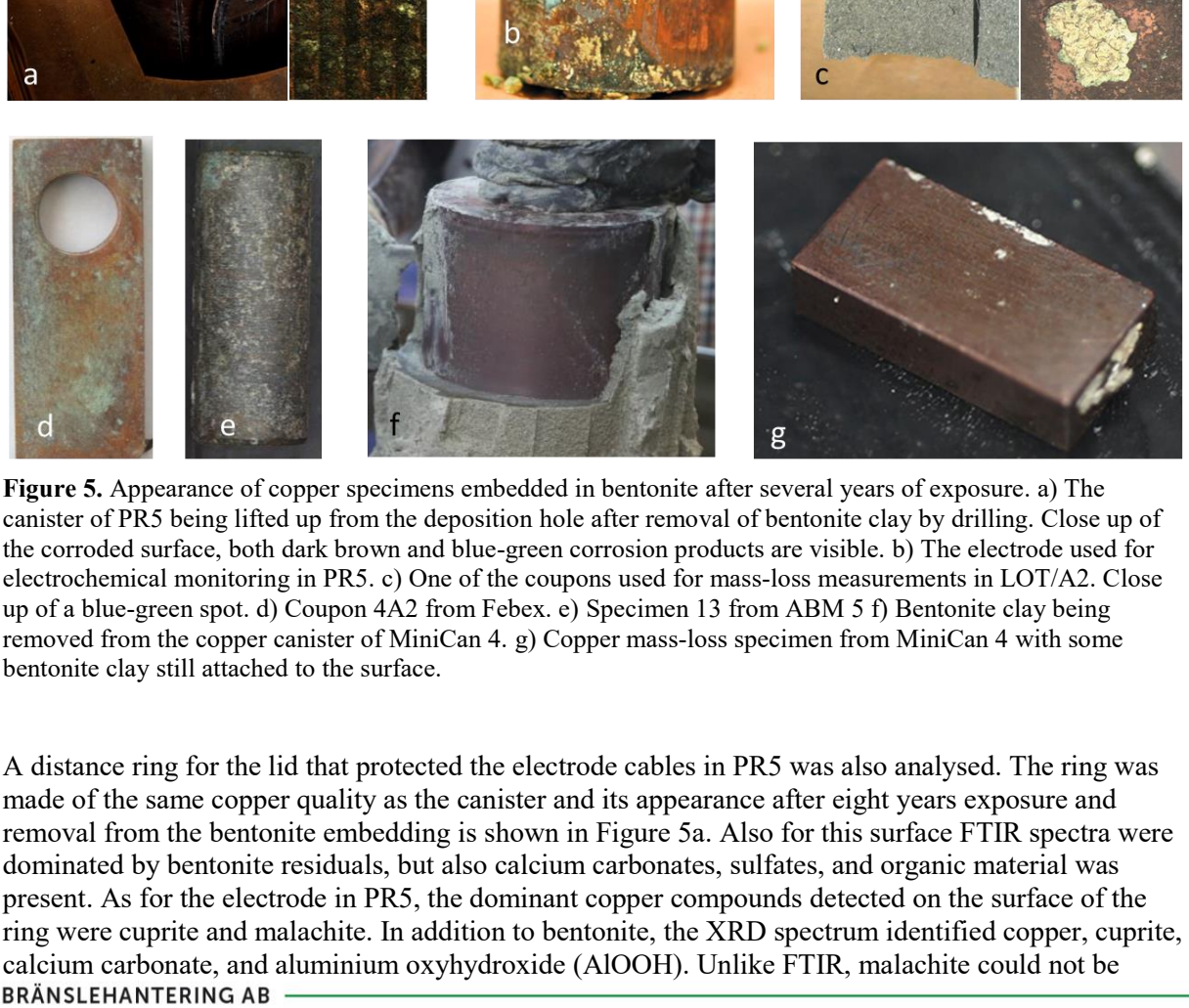

Figure 5. Appearance of copper specimens embedded in bentonite after several years of exposure. a) The canister of PR5 being lifted up from the deposition hole after removal of bentonite clay by drilling. Close up of the corroded surface, both dark brown and blue-green corrosion products are visible. b) The electrode used for electrochemical monitoring in PR5. c) One of the coupons used for mass-loss measurements in LOT/A2. Close up of a blue-green spot. d) Coupon 4A2 from Febex. e) Specimen 13 from ABM 5 f) Bentonite clay being removed from the copper canister of MiniCan 4. g) Copper mass-loss specimen from MiniCan 4 with some bentonite clay still attached to the surface.

A distance ring for the lid that protected the electrode cables in PR5 was also analysed. The ring was made of the same copper quality as the canister and its appearance after eight years exposure and removal from the bentonite embedding is shown in Figure 5a. Also for this surface FTIR spectra were dominated by bentonite residuals, but also calcium carbonates, sulfates, and organic material was present. As for the electrode in PR5, the dominant copper compounds detected on the surface of the ring were cuprite and malachite. In addition to bentonite, the XRD spectrum identified copper, cuprite, calcium carbonate, and aluminium oxyhydroxide (AlOOH). Unlike FTIR, malachite could not be

identified with XRD. A possible explanation for this inconsistency between FTIR and XRD, could be that the malachite crystals were too small or had too low crystallinity to be detected by XRD. The elemental composition of the corroded surfaces was qualitatively supported by GDOES (Glow Discharge Optical Emission Spectroscopy), which showed that oxygen was the dominant element (except copper), followed by silicon, aluminium and iron. No crystalline sulfide compounds could be identified with XRD or FTIR, however, sulfur was found with GDOES but in amounts orders of magnitude lower than oxygen (Taxén et al. 2012).

After breaking loose the copper coupons from the bentonite in LOT/A2/30, corrosion products were observed both on the copper coupon and on the bentonite surfaces facing the copper coupon (Figure 5c). A brown deposit with blue-green spots covered most of the copper coupons, although, areas with a metallic surface were also observed. When scraping off the brown corrosion product attached to the inner bentonite surface, blue-green corrosion products appeared, meaning that the blue-green product had formed on top of the brown product on the copper surface. XRD analysis confirmed that the main constituent of the brown surface deposit was cuprite and that the blue-green corrosion products contained paratacamite ($Cu_2(OH)_3Cl$). The blue-green corrosion product was not only unevenly distributed on the copper coupons, but also appeared in the clay adjacent to the coupons. SEM-EDS analysis revealed that the blue-green product in the clay had a higher content of Al, Si, and Fe, as compared to the adjacent surface on the coupon, meaning that these products had interacted chemically with the bentonite (Table A3-2 in Karnland et al. 2009). The higher chloride content of the blue-green spots, as compared with adjacent brown areas, supports the observation of paratacamite by XRD. While no copper sulfides were detected on the copper coupons with XRD or FTIR, particles rich in both copper and sulfur were identified at the copper-bentonite interface using SEM-EDS.

Copper specimens from ABM 5 have so far only been analysed for corrosion mass-loss (Section 3.3). The composition of the corrosion products will be analysed for the remaining copper specimens. Due to the similarity in experimental design and configuration, it is reasonable to presume that the corrosion product in ABM was similar to the LOT series (Gordon et al. 2018).

Table 2. Surface elemental composition of copper specimens in MiniCan 4 (EDS data from Appendix 10 in Gordon et al. 2017).

Sample/surface	O (wt%)	S (wt%)	O/S: mass	O/S: atoms
Cu electrode (5:1, point 5)	1.8	4.3	0.4	0.8
Cu electrode (6:1, analysis 1, point 6)	6.2	4.9	1.3	2.6
Cu electrode (6:1, analysis 1, point 7)	7.4	4.9	1.5	3.0
Cu electrode (6:1, analysis 2, point 4)	5.5	5.5	1.0	2.0
Cu mass loss (7:1, point 3)	3.0	5.6	0.5	1.0
Cu canister outer surface (25:1, analysis 1, point 3)	5.1	2.5	2.0	4.0
Cu canister outer surface (25:1, analysis 2, point 2)	3.5	2.7	1.3	2.6
Cu canister weld surface (26:1, point 4)	3.0	6.3	0.5	1.0
Cu canister weld surface (26:1, point 5)	2.6	2.6	1.0	2.0
Cu canister weld surface (26:1, cross section, point 4)	9.4	8.8	1.1	2.2
Average all samples/points	**4.8±2.3**	**4.8±1.9**	**1.0±0.5**	**2.0±1.0**

While the copper specimens of MiniCan 3 and 5 were not embedded in bentonite clay (and also contaminated by nearby corrosion of iron components) the copper specimens in MiniCan 4 were embedded in compact bentonite clay and were thus more comparable to copper surfaces in the other field tests. The surfaces of copper specimens in MiniCan 4 appeared to be covered with bentonite clay and a thin brown layer (Figures 5f and 5g). Raman spectroscopy was applied to several copper specimens, *e.g.* the outer canister surface and the mass-loss coupon, under strictly anoxic conditions and revealed mainly cuprite (Cu_2O) and sulfide, which was most likely chalchocite (Cu_2S). XRD was applied after some exposure to air and still showed cuprite and possibly some tenorite (CuO). Several copper surfaces in MiniCan 4 were examined regarding elemental composition using SEM-EDS (Appendix 10 in Gordon et al. 2017). Many of the analysed surfaces show bentonite as evident from the high content of Si, O, and Al. As bentonite contains oxygen, EDS spectra from these points do not

allow determination of the O/S ratio of the corrosion film. However, removing these data points and analysing bentonite free areas of the copper surfaces show that both the oxygen and sulfur contents were typically 2-9 wt.%. Notably, oxygen and sulfur occur in roughly similar amounts (wt.%) on the surfaces (Table 2). However, these numbers should be regarded as approximate, since there several factors complicating the interpretation of the EDS spectra, e.g. the semi-quantitative nature of EDS, the possibility that some Cu_2O formed during corrosion has been converted to Cu_2S, and adsorption of sulfate ions. Nevertheless, MiniCan is thus the only Äspö field test, in which a significant part of the corrosion was caused by sulfide. The explanation for this is that the residual amount of oxygen was smaller than in other field test (due to the smaller clay volume), that the flow of ground water was high at the location of MiniCan in the Äspö HRL, and that the ground water only had to diffuse through a few cm of bentonite clay to reach the copper surface.

The Febex experiment contained two copper specimens mounted in the bentonite clay close to the surface of the heater. The coupons have thus experienced high temperature (ca 100°C) during the 18 year long exposure. One of the specimens (4A2) was used for gravimetric determination of general metal loss, while the other (4A1) was used for surface examination and characterization of corrosion products. Both coupons had very similar appearance with a blue-green deposit covering large areas (Figure 5d). EDS spectra showed that the surface of coupon 4A1 was composed mainly of copper and oxygen. Brownish surfaces had a content of ca 20 wt% oxygen and traces of chloride, while blue-green areas had ca 40 wt% oxygen and a chloride content of ca 6 wt%. Elements from the bentonite clay were detected, but there were no indications of sulfur. The most plausible interpretation of the EDS data is thus that brownish surfaces were dominated by cuprite (Cu_2O), while blue-green deposits were composed of atacamite or paratacamite ($Cu_2(OH)_3Cl$). The presence of cuprite was confirmed by XRD.

In summary, the examination of copper surfaces from the field tests PR5, LOT/A2, MiniCan 4, and Febex, all resembling the KBS-3 concept in that the copper specimens were embedded in high density bentonite clay, shows that the corrosion in MiniCan 4 was less extensive (by mass-loss) and did not indicate any formation of Cu(II) corrosion products (Table 3). MiniCan 4 differed from the other experiments in two important aspects: it was at ambient temperature (ca 10°C) and it contained a very small amount of residual oxygen initially. In section 3.5 it will be analysed how these parameters might have affected the corrosion.

Table 3. Corrosion products identified on copper specimens from the test series LOT/A2, PR5, MiniCan 4, and Febex

Specimen	Technique	Corrosion Products	Reference
Febex/4A2, coupon	XRD, SEM-EDS	Cu_2O, $Cu_2(OH)_3Cl$	Wersin and Kober (2017)
PR5/C4 electrode	Raman, XRD, FTIR	Cu_2O, $Cu_2(OH)_2CO_3$	Rosborg (2013b)
PR5/lid distance ring	XRD, FTIR	Cu_2O, $Cu_2(OH)_2CO_3$	Taxén et al. (2012)
LOT/A2/30G coupon	XRD, SEM-EDS	Cu_2O, $Cu_2(OH)_3Cl$	Karnland et al. (2009)
MiniCan 4, coupon M4 7:1	Raman, SEM-EDS	Cu_2O, Cu_2S	Gordon et al. (2017)
MiniCan 4, canister surface	Raman, SEM-EDS	Cu_2O, Cu_2S	Gordon et al. (2017)

3.3 Corrosion depths determined by mass-loss

Gravimetric or mass-loss analysis of copper corrosion has been performed in several of the tests in MiniCan, LOT, ABM, and Febex. The average corrosion depth measured for a Febex copper specimen was ca 9 µm, while the depths from LOT and ABM varied between 2 and 5 µm, and all measurements in MiniCan were below 1 µm (Table 4). Mass-loss is a very robust method to quantify average corrosion depth since it does not invoke any assumptions about the corrosion process except that it occurs rather evenly over the surface.

Table 4. Gravimetric results and environmental parameters.

Coupon	T	t	Initial O_2	Buffer thickness	Mass- loss	Area	Average corr. depth	Integrated corr. rate	Reference
	°C	d	moles	cm	mg	cm^2	µm	µm y^{-1}	
Febex/4A2	100	6570	74	60	197	26.09	8.5	0.5	Wersin and Kober (2017)
LOT/S1/22A	50	487	0.8	8	80	24.5	3.7	3.1	Karnland et al. (2000)
LOT/A0/22A	80	710	0.8	8	86	20.25	4.8	2.4	Karnland et al. (2011)
LOT/A0/30C	35	710	0.8	8	83	20.25	4.6	2.4	Karnland et al. (2011)
LOT/A2/30G	30	2271	0.8	8	46	20.25	2.5	0.4	Karnland et al. (2009)
LOT/A2/30H	30	2271	0.8	8	27	20.25	1.5	0.2	Karnland et al. (2009)
ABM5/9	80	1825	0.8	8	43	9.5	5.0	1.0	Gordon et al. (2018)
ABM5/13	80	1825	0.8	8	19	9.5	2.3	0.5	Gordon et al. (2018)
ABM5/15	80	1825	0.8	8	25	9.5	2.9	0.6	Gordon et al. (2018)
ABM5/16	80	1825	0.8	8	23	9.5	2.7	0.5	Gordon et al. (2018)
MiniCan 3	15	1383	0.1	3	3.8	7.0	0.6	0.15	Smart et al. (2012)
MiniCan 4	15	3103	0.1	3	1.0	7.0	0.2	0.02	Gordon et al. (2017)
MiniCan 5	15	3103	0.1	-	5.9	7.0	0.9	0.11	Gordon et al. (2017)

3.4 Interpretation of integrated corrosion rates

Corrosion rates calculated as the measured corrosion depth (by mass-loss) divided by the whole exposure time, have been presented in several reports concerning the field tests discussed herein (Table 4). Important to note, these do not account for any changes in the corrosion process or mechanism due to changes in the environment during the exposure, and are thus not representative for the whole exposure period. In order to estimate the average corrosion rate under the initial aerobic period, information is needed regarding the amount of corrosion due to oxygen (and not sulfide), and the time it took for oxygen to be depleted.

In MiniCan 4, the integrated corrosion rate for the whole exposure period was 0.02 µm/y (Table 4). However, as was discussed above (Tables 2 and 3), both oxides and sulfides were present on the copper surfaces, and as it seems in similar amounts. Since it is known that O_2 was depleted within a few months (Section 3.1), it can be concluded that the initial oxygen driven corrosion must have occurred with an average rate that is much higher than 0.02 µm/y. For example, assuming that 50 % of the mass-loss was caused by O_2 corrosion, and that O_2 was depleted within 3 months, this would give an average corrosion rate of 0.4 µm/y during the first 3 months, i.e. twenty times higher than the integrated corrosion rate calculated for the whole exposure period of nearly 9 years. Consequently, the subsequent corrosion, most probably controlled by the diffusive transport of sulfide through the bentonite, must have occurred at a rate lower than the integrated corrosion rate for the whole exposure period. As mentioned in the discussion above when referring to Table 2, these numbers should be regarded as very approximate, since there are large uncertainties regarding the relative contributions of O_2 and sulfide driven corrosion. The calculation should not be used to predict corrosion rates during oxic or anoxic conditions, however, the example in the calculation serves to illustrate the principle problem with (and limited usefulness of) integrated corrosion rates when it is known that the corrosion process has changed during the exposure.

If the same corrosion process would have been dominating during the whole exposure periods of the field tests, i.e. if an oxidant was available at constant or similar concentration, the corrosion rate would have shown an exponential dependence on the temperature, as predicted by the Arrhenius equation. The relationship can be expressed as the logarithm of the rate plotted against the inverse temperature, which is then expected to give a linear plot (Figure 7). However, linear fitting of the logarithm of the nominal corrosion rates plotted against the inverse of the experimental temperature gave a very poor fit (R^2=0.28). The reason for the apparently weak relationship between the integrated corrosion rates and temperature, is to be found in the corrosion rates' poor representation for the whole exposure periods of the field tests, as discussed above.

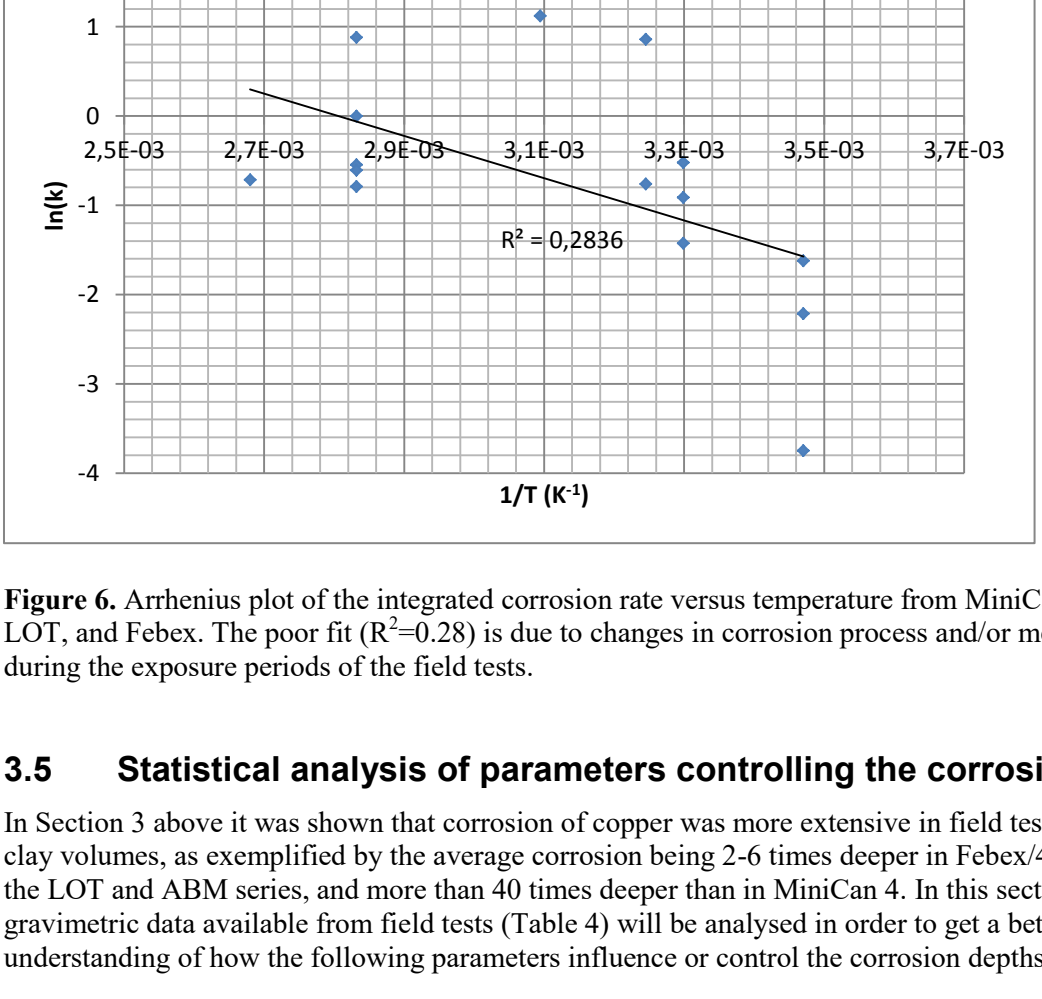

Figure 6. Arrhenius plot of the integrated corrosion rate versus temperature from MiniCan, ABM, LOT, and Febex. The poor fit (R^2=0.28) is due to changes in corrosion process and/or mechanism during the exposure periods of the field tests.

3.5 Statistical analysis of parameters controlling the corrosion

In Section 3 above it was shown that corrosion of copper was more extensive in field tests with large clay volumes, as exemplified by the average corrosion being 2-6 times deeper in Febex/4A2 than in the LOT and ABM series, and more than 40 times deeper than in MiniCan 4. In this section gravimetric data available from field tests (Table 4) will be analysed in order to get a better understanding of how the following parameters influence or control the corrosion depths measured:

- Temperature: measured as close as possible to the specific corrosion specimens.
- Time: taken as the total time of exposure in field, from installation to retrieval.
- Residual O_2: the total amount estimated as 1.3 moles O_2 per m^3 bentonite and contributions from initially air-filled gaps (see Section 3.1).
- Thickness of the bentonite buffer: used as an alternative estimate of O_2 available through diffusion.

In the first step, correlations between variables are analyzed. In the following steps, regression is used to elucidate the relative importance of the parameters. Possible outliers are excluded in a stepwise manner in order to further improve the understanding of which parameters that controlled the corrosion in these tests. The analysis was made using Statistica 12.0 and if nothing else is stated the statistical significance was set to a 95% confidence interval ($p<0.05$).

As the first step of analysis, a correlation matrix was set up for the parameters temperature, exposure time, residual O_2, corrosion depth and integrated corrosion rate. The analysis revealed relatively strong correlations of corrosion depth and temperature (R=0.73, Figure 7), as well as corrosion depth and residual O_2 (R=0.74, Figure 8). Both correlations were statistically significant.

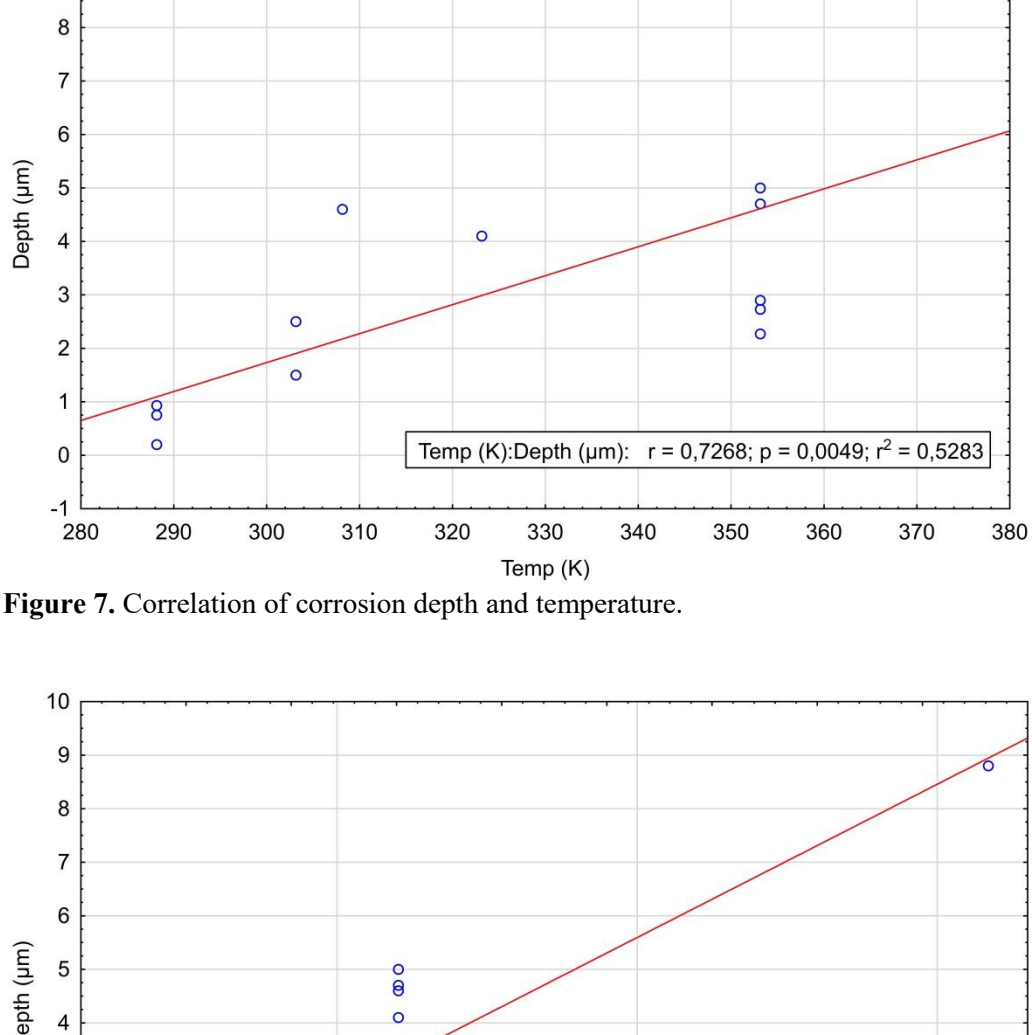

Figure 7. Correlation of corrosion depth and temperature.

Figure 8. Correlation of corrosion depth and residual O_2. The data is shown with a logarithmic x-axis in order to make the graph more readable, however, a linear fit was used to determine the correlation coefficient.

The correlation matrix also revealed a moderate but statistically significant negative correlation of the integrated corrosion rates with exposure time (R= -0.55). These three correlations are expected and understood. Residual O_2 is expected to control the corrosion on shorter time scales when no other oxidant (sulfide) is yet available. Higher temperature enhances the transport of O_2 to the copper surfaces, both by enhancing the diffusion rate of O_2 in water saturated clay, but also by drying out the heated zone which enhances convection of gases. The corrosion rate should decrease with time as O_2

is expected to be depleted on a timescale that is shorter than that required for sulfidic groundwater to become a significant contributor to corrosion.

However, the analysis also showed that there is a strong correlation of residual O_2 with time (R=0.84) as well as a moderate correlation between residual O_2 and temperature (R=0.46). These correlations have no physical meaning but are rather due to the experimental design; the longest exposures have been performed for the largest experiments, larger clay volume means larger amount of residual O_2, and the larger experiments have also been heated to higher temperatures. Another effect that comes into play here is that the larger and warmer experiments did not only contain more O_2 initially, but also, both the size and temperature makes the period required for water saturation of the clay longer, meaning that entrapped O_2 can be transported (via diffusion and convection) rapidly through the heated zone.

When linear regression analysis was performed on the whole set of data, i.e. including all gravimetric corrosion depths from Febex, LOT, ABM, and MiniCan in Table 4, temperature was found to be a relatively strong explanatory variable determining the corrosion depth (R^2=0.53, Table 6). The corresponding R^2 values for residual O_2 and bentonite thickness are 0.54 and 0.61, respectively. However, the explanatory degree of these variables depend to a some extent on the data point from Febex, in which the total amount of O_2 was much higher than in any other test. By excluding the Febex data from the linear regression analysis, temperature gets a slightly lower but still statistically significant explanatory degree of 43%, whereas residual O_2 only reduces to 57%. Thus, although the explanatory degree of temperature and O_2 when the whole data set is analyzed has some dependence on Febex, the dependence is not crucial.

Multiple regression analysis of the data set of Table 4, setting corrosion depth as the dependent variable and temperature, time, O_2, and bentonite thickness as independent variables, gave a total explanatory degree of 87%. Since the total amount of residual O_2 might not be available for corrosion of copper, especially not in Febex in which the diffusion distance is very long and since there was a large heated steel surface competing for O_2, it might be better to account for residual O_2 by approximating it with the bentonite thickness. Nevertheless, repeating the multiple regression analysis with the O_2 variable excluded had a very slight effect on the explanatory power of the model (R^2=0.86). Excluding both time and O_2, keeping only the temperature and bentonite thickness as independent variables, reduced the explanatory degree to 75%, which is still rather high.

As was discussed above in the linear regression analysis, the single data point from Febex could have an unbalanced influence on the data set. Therefore, a multiple regression analysis was performed on the data set with Febex excluded. The explanatory degree of the whole model now decreased from 87% to 79%, which is still rather high. Excluding O_2 among the independent variables, accounting for the available O_2 by the thickness of the bentonite instead, decreased the explanatory degree of the model further to 72%. It can thus be concluded that irrespective of whether Febex data is included or not in the analysis, and whether the availability of O_2 is described by the total amount of residual O_2 or the thickness of the bentonite clay, the most important variables determining the corrosion depth in the field tests are residual O_2 and temperature, as illustrated by the plot in Figure 9.

Table 5. Linear and multiple regression analysis of the gravimetric data set in Table 4. The values presented are coefficients of determination, R^2-values (in the text referred to as explanatory degree, in %). The abbreviation n.s. means not statistically significant, while n.a. means not applicable.

Type of regression	Corrosion depth vs				
	Temperature	Time	Residual O_2	Bentonite thickness	Whole model
Linear; all data	0.53	n.s.	0.54	0.61	n.a.
Linear: -Febex	0.42	0.54	0.57	0.51	n.a.
Multiple; all data	n.a.	n.a.	n.a.	n.a.	0.87
Multiple; -O_2	n.a.	n.a.	n.a.	n.a.	0.86
Multiple; -O_2, -time	n.a.	n.a.	n.a.	n.a.	0.75
Multiple; -Febex	n.a.	n.a.	n.a.	n.a.	0.79
Multiple; -Febex, - O_2	n.a.	n.a.	n.a.	n.a.	0.72

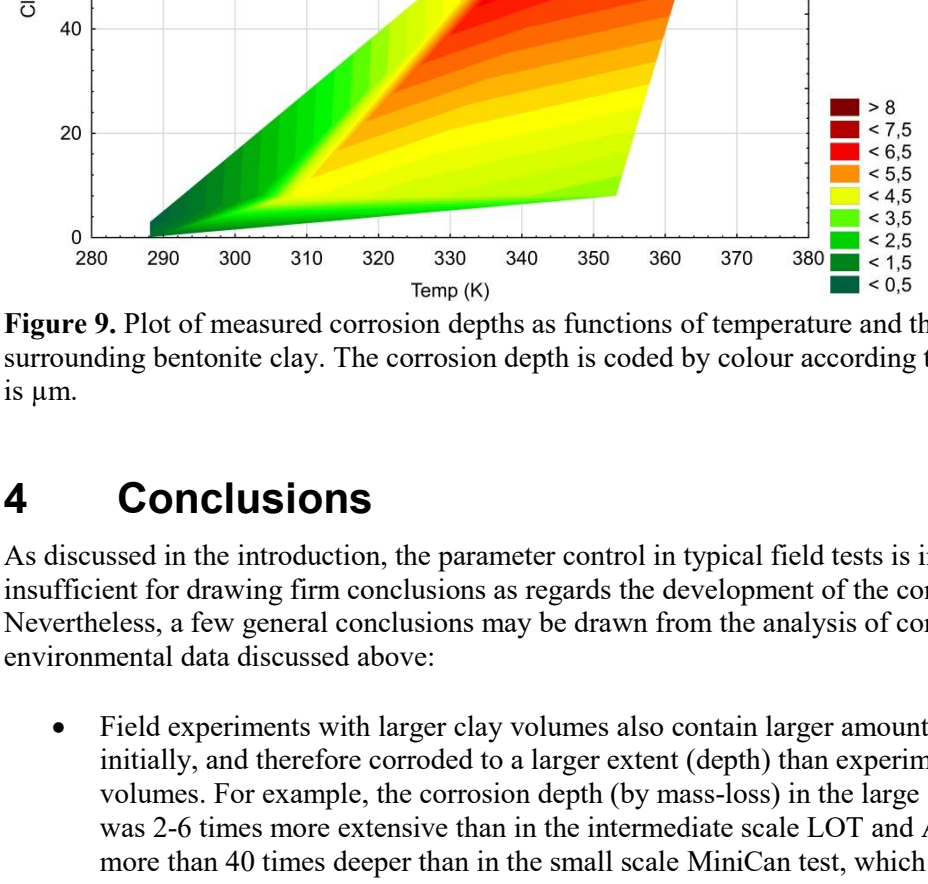

Figure 9. Plot of measured corrosion depths as functions of temperature and thickness of the surrounding bentonite clay. The corrosion depth is coded by colour according to the scale and the unit is µm.

4 Conclusions

As discussed in the introduction, the parameter control in typical field tests is in many cases insufficient for drawing firm conclusions as regards the development of the corrosion process. Nevertheless, a few general conclusions may be drawn from the analysis of corrosion and environmental data discussed above:

- Field experiments with larger clay volumes also contain larger amounts of residual oxygen initially, and therefore corroded to a larger extent (depth) than experiments with smaller clay volumes. For example, the corrosion depth (by mass-loss) in the large scale experiment Febex was 2-6 times more extensive than in the intermediate scale LOT and ABM experiments, and more than 40 times deeper than in the small scale MiniCan test, which contained very little residual oxygen due to its small clay volume.

- In experiments with larger clay volumes and larger amounts of residual oxygen, i.e. LOT, Prototype, and Febex, divalent oxygen containing corrosion products are observed, e.g. $Cu_2(OH)_3Cl$.

- In experiments with small amounts of residual oxygen, i.e. the MiniCan series, O_2 was depleted within a few months from the start of the experiment and only monovalent copper oxide (Cu_2O) was observed.

- While both Cu_2S and Cu_2O were observed spectroscopically and the elements O and S occurred in similar amounts on the copper surfaces in MiniCan, only small amounts of sulfur rich particles were detected in LOT, only traces of sulfur were found in Prototype, while no sulfur was detected on the copper specimens in Febex.

- In the field experiments reviewed, the measured corrosion depths correlated well with both the amount of residual O_2 and temperature. It is thus concluded that the corrosion of copper under repository like initial conditions is controlled primarily by residual O_2 and temperature.

- In the conceptual corrosion model employed in SKB's safety assessments, the early corrosion is controlled by mass-balance of oxygen, while the subsequent long-term sulfide corrosion is controlled by sulfide transport limitations, i.e. the low sulfide concentration in the ground water and diffusion through the bentonite clay. This conceptual model is compatible with the results of the field experiments reviewed and analyzed herein.

References

SKB's (Svensk Kärnbränslehantering AB) publications can be found at www.skb.com/publications.

Birgersson M, Goudarzi R, 2018. Investigations of gas evolution in an unsaturated KBS-3 repository. SKB TR-18-11, Svensk Kärnbränslehantering AB.

Giroud N, 2014. FEBEX – assessment of redox conditions in phase 2 before dismantling. Nagra Arbeitsbericht NAB 14-55, Nagra, Switzerland.

Gordon A, Sjögren L, Taxen C, Johansson A J, 2017. Retrieval and post-test examination of packages 4 and 5 of the MiniCan field experiment. SKB TR-16-12, Svensk Kärnbränslehantering AB.

Gordon A, Pahverk H, Börjesson E, Johansson A J, 2018. Examination of copper corrosion specimens from ABM 45, package 5. SKB TR-18-17, Svensk Kärnbränslehantering AB.

Karnland O, Sandén T, Johannesson L-E, Eriksen T, Jansson M, Wold S, Pedersen K, Motamedi M, Rosborg, B, 2000. Long term test of buffer material. Final report on the pilot parcels. SKB TR-00-22, Svensk Kärnbränslehantering AB.

Karnland O, Olsson S, Dueck A, Birgersson M, Nilsson U, Heman-Håkansson T, Pedersen K, Nilsson S, Eriksen T, Rosborg B, 2009. Long term test of buffer material at the Äspö Hard Rock Laboratory, LOT project. Final report on the A2 test parcel. SKB TR-09-29, Svensk Kärnbränslehantering AB.

Karnland O, Olsson S, Sandén T, Fälth B, Jansson M, Eriksen T, Svärdström K, Rosborg B, 2011. Long term test of buffer material at the Äspö HRL, LOT project. Final report on the A0 test parcel. SKB TR-09-31, Svensk Kärnbränslehantering AB.

King F, Lilja C, Vähänen M, 2013. Progress in the understanding of the long-term corrosion behaviour of copper canisters. Journal of Nuclear Materials 438, 228–237.

King F, Chen J, Qin Z, Shoesmith D, Lilja C, 2017. Sulphide-transport control of the corrosion of copper canisters. Corrosion Engineering, Science and Technology 52, 210–216.

Lanyon G W, Gaus I, 2016. Main outcomes and review of the FEBEX In Situ Test (GTS) and Mock-up after 15 years of operation. Nagra Technischer Bericht NTB 15-04, Nagra, Switzerland.

Rosborg, 2013a. Recorded corrosion rates on copper electrodes in the Prototype Repository at the Äspö HRL. SKB R-13-13, Svensk Kärnbränslehantering AB.

Rosborg, 2013b. Post-test examination of a copper electrode from deposition hole 5 in the Prototype Repository. SKB R-13-14, Svensk Kärnbränslehantering AB.

Rosborg B, Eden D, Karnland O, Pan J, Werme L, 2004. Real-time monitoring of copper corrosion at the Äspö HRL. In Féron D, Macdonald D D (eds). Prediction of long term corrosion behaviour in nuclear waste systems: proceedings of the 2nd International Workshop Organized by the Working Party on Nuclear Corrosion (WP4) of the European Federation of Corrosion (EFC), Nice, September 2004 (EUROCORR'2004). Chatenay-Malabry, France: Andra, 11–23.

Rosborg B, Kosec T, Kranjc A, Kuhar V, Legat A, 2012. The corrosion rate of copper in a bentonite test package measured with electric resistance sensors. SKB R-13-15, Svensk Kärnbränslehantering AB.

Sandén T, Nilsson U, Andersson L, Svensson D, 2018. ABM45 experiment at Äspö Hard Rock Laboratory. Installation report. SKB P-18-20, Svensk Kärnbränslehantering AB.

SKB, 2010. Corrosion calculations report for the safety assessment SR-Site. SKB TR-10-66, Svensk Kärnbränslehantering AB.

Smart N R, Rance A P, 2009. Miniature canister corrosion experiment – results of operations to May 2008. SKB TR-09-20, Svensk Kärnbränslehantering AB.

Smart N, Rance A, Reddy B, Fennell P, Winsley R, 2012. Analysis of SKB MiniCan Experiment 3. SKB TR-12-09, Svensk Kärnbränslehantering AB.

Smart N, Reddy B, Nixon D, Rance A, Johansson A J, 2015. A Miniature Canister (MiniCan) Corrosion experiment. Progress report 5 for 2008–2013. SKB P-14-19, Svensk Kärnbränslehantering AB.

Smith J, Qin Z, Shoesmith D, King F, Werme L, 2004. Corrosion of copper nuclear waste containers in aqueous sulphide solutions. MRS Online Proceedings Library 824, Scientific Basis for Nuclear Waste Management XXVIII.

Smith J, Qin Z, King F, Werme L, Shoesmith D W, 2007a. Sulfide film formation on copper under electrochemical and natural corrosion conditions. Corrosion 63, 135–144.

Smith J, Wren J C, Odziemkowski M, Shoesmith D W, 2007b. The electrochemical response of preoxidized copper in aqueous sulfide solutions. Journal of The Electrochemical Society 154, C431–C438.

Svemar C, Johannesson L-E, Grahm P, Svensson D, Kristensson O, Lönnqvist M, Nilsson U, 2016. Prototype Repository Opening and retrieval of outer section of Prototype Repository at Äspö Hard Rock Laboratory**.** Summary report. SKB TR-13-22, Svensk Kärnbränslehantering AB.

Taxén C, Lundholm M, Person D, Jakibsson D, Sedlakova M, Randelius M, Karlsson O, Rydgren P, 2012. Analyser av koppar från prototypkapsel 5 och 6. SKB P-12-22, Svensk Kärnbränslehantering AB. (In Swedish.)

Wersin P, Kober F (eds), 2017. FEBEX-DP. Metal corrosion and iron–bentonite interaction studies. Nagra Arbeitsbericht NAB 16-16, Nagra, Switzerland.